Targeting the DNA Damage Response Pathways and Replication Stress in Colorectal Cancer

Erika Durinikova[1], Nicole M. Reilly[1,2], Kristi Buzo[1,2], Elisa Mariella[1,2], Rosaria Chilà[2,3], Annalisa Lorenzato[1,2], João M. L. Dias[4,5], Gaia Grasso[1,2], Federica Pisati[6], Simona Lamba[1], Giorgio Corti[1,2], Andrea Degasperi[4,5], Carlotta Cancelliere[1], Gianluca Mauri[3,7], Pietro Andrei[1,2], Michael Linnebacher[8], Silvia Marsoni[3], Salvatore Siena[7,9], Andrea Sartore-Bianchi[7,9], Serena Nik-Zainal[4,5], Federica Di Nicolantonio[1,2], Alberto Bardelli[1,2], and Sabrina Arena[1,2]

ABSTRACT

Purpose: Genomic instability is a hallmark of cancer and targeting DNA damage response (DDR) is emerging as a promising therapeutic strategy in different solid tumors. The effectiveness of targeting DDR in colorectal cancer has not been extensively explored.

Experimental Design: We challenged 112 cell models recapitulating the genomic landscape of metastatic colorectal cancer with ATM, ATR, CHK1, WEE1, and DNA-PK inhibitors, in parallel with chemotherapeutic agents. We focused then on ATR inhibitors (ATRi) and, to identify putative biomarkers of response and resistance, we analyzed at multiple levels colorectal cancer models highly sensitive or resistant to these drugs.

Results: We found that around 30% of colorectal cancers, including those carrying *KRAS* and *BRAF* mutations and unresponsive to targeted agents, are sensitive to at least one DDR inhibitor. By investigating potential biomarkers of response to ATRi, we found that ATRi-sensitive cells displayed reduced phospho-RPA32 foci at basal level, while ATRi-resistant cells showed increased RAD51 foci formation in response to replication stress. Lack of *ATM* and *RAD51C* expression was associated with ATRi sensitivity. Analysis of mutational signatures and HRDetect score identified a subgroup of ATRi-sensitive models. Organoids derived from patients with metastatic colorectal cancer recapitulated findings obtained in cell lines.

Conclusions: In conclusion, a subset of colorectal cancers refractory to current therapies could benefit from inhibitors of DDR pathways and replication stress. A composite biomarker involving phospho-RPA32 and RAD51 foci, lack of ATM and RAD51C expression, as well as analysis of mutational signatures could be used to identify colorectal cancers likely to respond to ATRi.

Introduction

DNA damage response (DDR) pathways play a critical role for the growth and survival of cancer cells, and their aberrant regulation is responsible for genomic instability, a well-known cancer hallmark (1). Five major repair pathways including homologous recombination (HR), non-homologous end-joining (NHEJ), base excision repair (BER), nucleotide excision repair, and DNA mismatch repair (MMR) are modulated by more than 450 different effectors which are involved in the repair of single-nucleotide defects or DNA single-strand and double-strand breaks (2). Several studies have already elucidated the role of HR defects and their clinical implications in cancers such as those of ovarian, breast, prostate, and pancreatic origin (3). In light of the cross-talk between DNA damage sensing, repair, and cell-cycle checkpoints, a set of DDR inhibitors (DDRi) targeting essential DNA repair pathways was recently developed following the paradigmatic example of PARP (Poly(ADP)-ribose polymerase) inhibition in *BRCAness*-affected cancers (4). Replication stress (RS) represents a cause of DNA damage (5) and elevated levels of RS are often observed in cancer cells, mostly attributed to the presence of oncogenic signaling or to the aberrant regulation of cell-cycle checkpoint activators. Therefore, RS, together with defective DDR, represent a therapeutic opportunity in cancers (6, 7).

Colorectal cancer is the third leading cause for cancer-related death in the Western world and current classification based on loss of a specific DDR function encompasses the distinction into microsatellite stable (MSS) and unstable (MSI) colorectal cancers (8). A subset of colorectal cancer with MSI-high or deficient MMR profiles are effectively treated with immune checkpoint inhibitors (9), while MSS colorectal cancers are mainly subjected to one-size-fits-all chemotherapeutic regimen, often exposing patients to known risk of iatrogenic toxicity in exchange of an unknown chance of clinical benefit. We and others have shown that several targeted agents, including EGFR, HER2, TRK, and BRAF inhibitors, are effective in subsets of patients with MSS colorectal cancer, but response is generally transient owing to the emergence of acquired resistance (10). Moreover, for both patients with MSI and MSS colorectal cancer, available treatments

[1]Candiolo Cancer Institute, FPO - IRCCS, Candiolo, Torino, Italy. [2]Department of Oncology, University of Torino, Candiolo, Italy. [3]IFOM ETS - The AIRC Institute of Molecular Oncology, Milan, Italy. [4]Department of Medical Genetics, University of Cambridge, Cambridge, United Kingdom. [5]Early Cancer Institute, University of Cambridge, Cambridge, United Kingdom. [6]Histopathology Unit, Cogentech, Milan, Italy. [7]Department of Oncology and Hemato-Oncology, University of Milan, Milan, Italy. [8]Clinic of General Surgery, Molecular Oncology and Immunotherapy, University of Rostock, Rostock, Germany. [9]Niguarda Cancer Center, Grande Ospedale Metropolitano Niguarda, Milan, Italy.

A. Bardelli and S. Arena contributed as co-senior authors to this article.

Corresponding Authors: Sabrina Arena, Candiolo Cancer Institute, FPO – IRCCS and Department of Oncology, University of Torino, Strada Provinciale 142, km 3.95, Candiolo 10060, Torino, Italy. Phone: 39-011-9933223; E-mail: sabrina.arena@unito.it; and Alberto Bardelli, Phone: 39-011-9933235; E-mail: alberto.bardelli@unito.it

Clin Cancer Res 2022;28:3874–89

doi: 10.1158/1078-0432.CCR-22-0875

Translational Relevance

The identification of novel effective therapies for patients with colorectal cancer that cannot benefit from targeted or immune treatment represents a pressing need in oncology. Defects in effectors involved in the DNA damage response (DDR) and replication stress response might constitute a potentially targetable vulnerability that has led to the development of new agents (DDR inhibitors, DDRi), currently under phase I–III testing. In this work, we test the sensitivity to seven different types of DDRi in a platform including 112 cell lines representing the molecular landscape of colorectal cancer and in a subset of colorectal cancer organoids. Of note, we identify that up to 30% of colorectal cancer models are sensitive to at least one DDRi and we suggest that the use of a composite biomarker involving phospho-RPA32 and RAD51 foci analysis, lack of ATM and RAD51C expression, as well as HRDetect analysis could better stratify colorectal cancers likely to benefit from ATR inhibitors.

beyond second-line regimen remain limited owing to the low efficacy and high toxicity burden (11).

Recent works suggest that colorectal cancers carrying defective DNA repair pathways might be amenable to PARP therapeutic targeting (12–14) or drugs targeting RS (15–17), although identification of reliable biomarkers of response and/or stratification approaches still remain a pressing need.

Here, we sought to explore in a more systematic and extended way the efficacy of targeting DDR in colorectal cancer by screening 112 cell lines recapitulating the molecular landscape of colorectal cancer with seven different DDRi. Around 30% of colorectal cancer cell models demonstrated sensitivity to at least one DDRi with addition of observed sensitive pattern to RS inhibitors also in a subset of patient-derived organoids (PDO). In addition, we show how alterations of DDR effectors and the analysis of mutational signatures could be exploited as a "composite" biomarker to identify patients likely to benefit from ATR inhibitors (ATRi), a class of drugs that are currently under advanced clinical development and show efficacy also as monotherapy (18). Parallel analysis of response to chemotherapeutic agents pinpoints cross-sensitivities with clinically relevant implications.

Materials and Methods

Cell lines and cell authentication

Colorectal cancer cell lines as a part of our biobank were characterized previously (refs. 12, 19, 20; Supplementary Table S1). Each cell line was cultured in its specific media under standard culture conditions and routinely checked for *Mycoplasma* contamination (PCR *Mycoplasma* Detection Kit; ABM). Genetic identity was performed before drug testing and key molecular assays by using the PowerPlex 16 HS System (Promega) through short tandem repeats at 16 different loci (D5S818, D13S317, D7S820, D16S539, D21S11, vWA, TH01, TPOX, CSF1PO, D18S51. D3S1358, D8S1179, FGA, Penta D, Penta E, and amelogenin). Amplicons from multiplex PCRs were separated by capillary electrophoresis (3730 DNA Analyzer; Applied Biosystems) and analyzed using GeneMapperID v.3.7 software (Life Technologies).

DDRi and chemotherapeutic drugs

5-fluorouracil (5-FU; S1209), oxaliplatin (S1224), SN-38 (S4908), and olaparib (AZD2281, Ku-0059436, S1060) were purchased from Selleckchem. Berzosertib (ATRi; HY-13902), ceralasertib (ATRi; HY-19323), rabusertib [CHK1 inhibitor (CHKi); HY-14720], adavosertib [Wee1 inhibitor (Wee1i); HY-10993], AZD0156 [ATM inhibitor (ATMi); HY-100016], and nedisertib [DNA-PK inhibitor (DNA-PKi); HY-101570] were purchased from MedChemExpress, while MG-132 (474790) was purchased from Merck and hydroxyurea (HU; H8627) from Sigma.

Chemotherapy and DDRi screening

The sensitivity was tested in a 7-day-long proliferation assay. Cells were seeded in 48-well culture plates in different numbers per well depending on a cell line to reach 80%–90% confluency of control wells in the end of the assay. The following day, serial dilutions of oxaliplatin (0.75–12 μmol/L), 5-FU (0.625–10 μmol/L), SN-38 (1–150 nmol/L), berzosertib (0.65–3 μmol/L), ceralasertib (0.215–10 μmol/L), rabusertib (0.1–5 μmol/L), adavosertib (0.65–3 μmol/L), AZD-0156 (0.32–15 μmol/L), and nedisertib (0.43–20 μmol/L) were added using the Tecan D300e Digital Dispenser. Seven days later, the cell viability was assessed by Cell TiterGlo Luminescent Cell Viability assay (Promega) and measured by the Tecan SPARK M10 plate reader. Viability measured for each treatment condition was normalized to untreated controls. Final data are an average of at least three biological replicates with calculated AUC values. To rank cells' response within each particular drug, we calculated Z score values based on the standard formula.

Genomic DNA extraction, whole-exome sequencing, and bioinformatic analysis

Genomic DNA samples were extracted from each cell line using Maxwell RSC Blood DNA Kit (Promega) and sent to IntegraGen (France) for sequencing. Data analysis was performed in-house following procedures described previously (21).

RNA extraction, sequencing, and bioinformatic analysis

RNA samples were extracted using Maxwell RSC miRNA Tissue Kit (Promega). RNA sequencing (RNA-seq) reads in FASTQ format were aligned to the hg38 version of the human genome using the splice-aware MapSplice aligner. Output BAM files were processed to translate genomic coordinates into transcriptomic ones and remove reads with indels, large inserts, and zero mapping quality before proceeding with transcript and gene quantification using RSEM and GENCODE Release 33 as human gene annotation. In particular, we computed robust fragments per kilobase of transcript per million mapped reads (FPKM) values exploiting the tximport R Bioconductor package (22) and the FPKM function included in the DESeq2 R Bioconductor package (23) starting from RSEM gene-level expected counts and effective lengths obtained for each gene in each sample. The resulting gene expression matrix was subsequently annotated with gene names from the GENCODE annotation file and filtered by applying the following criteria: (i) genes on chrM or chrY pseudoautosomal regions were removed; (ii) genes with FPKM $= 0$ in >90% analyzed samples or FPKM < 1 in all analyzed samples were considered not expressed and removed; (iii) only protein-coding genes, as defined by the GENCODE annotation file, were selected for subsequent analysis.

Prediction of molecular subtypes

The prediction of CMS and CRIS molecular subtypes was performed after $\log_2$ transformation of gene expression values using the CMScaller R package and the CRIS classifier R package with default parameters. Cell lines that cannot be confidently assigned to a single subtype (FDR > 5%) were labeled as NA (not available).

MSI analysis

The MSI status was evaluated as described previously (12).

Circos plot generation

Circular representation of colorectal cancer molecular features was generated by combining functions of R packages circlize and ComplexHeatmap (24, 25).

Whole-genome sequencing and mutational signature analysis

Genomic DNA samples were extracted using ReliaPrep gDNA Tissue Miniprep System (Promega) and sent to IntegraGen (France) for sequencing. Raw reads were aligned to the human reference genome GRCh37/hg19 by BWA-MEM (26) and the resulting BAM files were used as input for the pipeline developed to assess mutational signatures on colorectal cancer cell lines (without matched normal). Germline small [single-nucleotide variants (SNV) and Indels] and structural variants (SV) were first detected with Strelka (version 2.9.10; ref. 27) and Manta (version 1.6.0; ref. 28), executed on tumor-only mode, using default parameters. Variants with "PASS" filter flag were taken into the next step. Common SNVs and Indels located within a genomic window of common Indels that started 4 bp upstream and ended 4 bp downstream were removed along with recurrent variants in the cohort. SVs were discarded if fully located within the same genomic region of common SVs from the same class (tandem duplications, deletions, inversions, and translocations). So-called common variants were compiled from four databases available in the literature (29–32).

Copy-number alterations (CNA) were called with ASCAT (33) using read counts at genomic positions present in 1000 Genome SNPs (phase III, release 83; ref. 34). Read counts from tumor samples were normalized using read count medians of all colorectal cancer cell lines at each genomic position.

Mutational signature analysis was performed using SignatureTools software package (35) on the filtered variants. SignatureExtraction (35) algorithm was adapted to additionally extract base substitution signatures that have not been classified as known signatures but are present in these unmatched colorectal cancer cell lines. Variants r in these "novel" signatures are likely to represent outstanding germline variants or artifacts introduced in the various steps of cell line culturing and sequencing that were not discarded in previous steps. Cosmic base substitution signatures (v3.2; ref. 36) 1, 2, 3, 5, 6, 7a, 7b, 8, 10a, 10b, 11, 13, 14, 15, 17a, 17b, 18, 20, 26, 28, 30, 36, 37, 40, 44, known to be associated with DDR pathways or observed in colorectal cancer, were considered on signature extraction with SignatureFit. The two "novel" signatures were also added to the list to allow an independent extraction of signature associated with outstanding germline variants and artifacts.

The HRDetect model suitable for mutational signature analysis carried out with samples without matched normal using tumor variants and CNA calls filtered with the pipeline described above was derived on the same training and validation dataset of the original model (37). In this case, only one "novel" signature was added to represent outstanding germline variants. The resulting HRDetect model predicted BRCA1/BRCA2 deficiency with a sensitivity and specificity of approximately 91% in 560 breast cancers for a probabilistic cutoff of 0.5. The same model was used to estimate HRDetect score in the colorectal cancer cell lines.

CRISPR-mediated *ATM* knockout

To knockout (KO) *ATM* in SW480 cell line, we used the genome editing one vector system (lentiCRISPR-v2; Addgene #52961). Single-guide RNAs (sgRNA) were designed using the CRISPR tool (http://crispr.mit.edu) and the following sgRNA sequences were used: sgRNA1: CCAAGGCTATTCAGTGTGCG; sgRNA2: TGATAGAGCTACAGAACGAA. Annealed sgRNA oligonucleotides targeting mouse *ATM* were cloned into Bsmbl lentiCRISPR-v2 plasmid, as described previously (38). SW480 cells were transfected with lentiCRISPR-v2 vector plasmid (using the same guides as described above). Transfection was carried out using Lipofectamine 3000 (Life Technologies) and Opti-MEM (Invitrogen), according to the manufacturer's instructions. After 48 hours, cells were incubated with puromycin (Sigma-Aldrich) for 4 days and subsequently single-cell diluted in 96-well plates. We selected clones that lacked ATM and confirmed the absence of the protein and Cas9 based on Western blot analysis. Testing of ATM KO clones with berzosertib and ceralasertib was performed in 96-well plates, where cells were treated for 6 days at the indicated concentrations and cell viability was assessed by Cell TiterGlo Luminescent Cell Viability assay (Promega). Treated wells were normalized to untreated wells. Final results are expressed as an average of three biological replicates.

Immunofluorescence

Cells seeded at a density of 1–2 $\times$ 10^5 cells on a glass coverslip in a 24-well plate were treated the next day with HU at a concentration of 2.5 mmol/L for indicated times. At the end of treatment, cells were fixed in 4% paraformaldehyde for 20 minutes at room temperature and permeabilized with 0.1% Triton-X100 in PBS for 5 minutes. Cells were incubated at room temperature with 1% BSA in PBS for 30 to 60 minutes, followed by incubation overnight at 4°C with the following primary antibodies diluted in PBS containing 1% of BSA: anti-phospho-RPA32 (Ser33; Bethyl Laboratories A300-246A; 1:500), anti-phospho-CHK1 (Ser345; Cell Signaling Technology 2348S; 1:400), anti-phospho-Histone H2AX (Ser139; Bethyl Laboratories A300-081A; 1:600), anti-RAD51 (Millipore ABE257; 1:100). After washing, cells were fluorescently labeled with an Alexa Fluor 555 or Alexa Fluor 488 donkey anti-rabbit antibody (Molecular Probes; 1:400) for 1 to 2 hours at room temperature. Nuclei were stained with DAPI. A Leica DMI6000B fluorescence microscope (Leica Microsystems) under a 40$\times$ dry objective was used to detect pRPA32, pCHK1, γH2AX, and RAD51 foci or pan-nuclear staining. For detection of nuclear-localized foci, images were captured at 10 individual z-planes and were merged using the "Z Project" function in ImageJ. Individual nuclei were scored for foci positivity as identified based upon signal intensity above general background staining levels and present within the nucleus as assessed by DAPI staining. Cells containing $\geq$ 5 distinct foci were defined as foci positive, and the percentage of positive nuclei was calculated as [(number of foci-positive nuclei)/(number of nuclei scored)]*100. For pan-nuclear staining, images were captured at the focal plane. Individual nuclei were scored for positivity using the ImageJ "analyze particles" function and the percentage of positive nuclei was calculated as [(number of foci-positive nuclei)/(number of nuclei scored)]*100. A minimum of 400 nuclei per sample were scored.

Olaparib screening

The response to olaparib in a long-term proliferation assay (10–14 days) was retrieved from our previous publication (12). For all the cell lines which were not tested previously, we provided the very same experimental setup.

Organoid culture and drug screening

Tumor samples were obtained from patients treated at Niguarda Cancer Center (Milan, Italy) after written consent and the study was

conducted in accordance with the local Independent Ethical Committee (protocol 194/2010). The PDOs and patient-derived xenoorganoids were established and maintained in the culture as described in full details in ref. 12.

Organoids were enzymatically dissociated using TrypLE Express Enzyme for 10 to 20 minutes at 37°C to obtain single-cell suspensions and seeded at a density of 4,000 to 6,000 cells per well in 96-well plates precoated with basement membrane extract (BME; Cultrex BME Type 2; Amsbio) overlayed with 100 μL of growth media containing 2% BME. The treatment with drugs started on day 4 after seeding when formed growing organoids were visible. Organoids were treated in fresh 150 μL medium containing 2% BME with increasing doses of six different DDRi or SN-38 in technical quadruplicates, covering physiologic concentrations of the drugs. Treatment was done automatically by Tecan D300e Digital Dispenser. A total of 4 μmol/L MG-132 was used as a positive control; DMSO served as negative control. The viability was assayed at the end of the experiment after 7 days of treatment by CellTiter-Glo Luminescent Cell Viability assay (Promega) with modifications. Briefly, plates were equilibrated at room temperature for 30 minutes and reagent was mixed 1:1 with organoid media. Organoids were then subjected to the lysis by vigorous shaking for 25 minutes, and readout was done by plate reader Tecan SPARK 10M. The raw CTG values were normalized to the mean of the DMSO control wells on a per-plate basis. The control wells (positive and negative) were used to calculate *Z* factors to indicate the quality of the data generated in the screening plate (as a standard rule, data obtaining *Z* factor >0.4 are acceptable). All experiments were independently repeated at least two times, and final results are expressed as an average of biological replicates.

The formula used to calculate *Z* factor:

$$Z\ factor = 1 - \frac{3 * standard\ deviation(negative\ control) + 3 * standard\ deviation(positive\ control)}{average(negative\ control) - average(positive\ control)}$$

Immunofluorescence in organoids

Untreated and HU-treated (at a concentration of 2.5 mmol/L for 24 hours) organoids, grown on chamber slides (Falcon Culture-Slides) previously precoated with BME, were fixed in 4% paraformaldehyde in PBS solution for 30 minutes at room temperature and permeabilized with 0.5% Triton-X100 in PBS for 30 minutes at room temperature. Organoids were then incubated with 1% BSA in PBS for 60 minutes, followed by incubation overnight with the following primary antibodies diluted in PBS containing 1% of BSA and 1% of donkey serum: anti-RAD51 (Millipore ABE257; 1:100), anti-phospho-RPA32 (Ser33; Bethyl Laboratories A300-246A; 1:500), and anti-phospho-Histone H2AX (Ser139; Bethyl Laboratories A300-081A; 1:600). After washing, organoids were fluorescently labeled with Alexa Fluor 488 donkey anti-rabbit antibody (Invitrogen) diluted 1:400 in PBS containing 1% BSA and 1% donkey serum for 1 to 2 hours. Nuclei were stained with DAPI. Slides were then mounted using the fluorescence mounting medium (Dako) and analyzed using a confocal laser scanning microscope (TCS SPE II, Leica).

IHC in cell lines and organoids

For IHC analyses, biological samples were sliced in 4-μm-thick sections, deparaffinized in xylene, and rehydrated through decreasing concentrations (100%, 95%, 80%, and 70%) of ethyl alcohol, then rinsed in distilled water. Antigen retrieval was carried out using preheated target retrieval solution for 30 minutes. Endogenous peroxidase activity was quenched with 0.3% hydrogen peroxide in distilled water. Slides were treated with 1% BSA and 2% FBS in PBS and then incubated in a closed humid chamber overnight at 4°C with anti-RAD51C (1:1,000, Thermo Fisher Scientific, PA5-75307) or anti-ATM antibody (1:100 in case of cell lines; 1:500 in case of PDOs, Abcam ab32420). The antibody binding was detected using a polymer detection kit (GAR-HRP, Microtech) followed by a diaminobenzidine chromogen reaction (Peroxidase substrate kit, DAB, SK-4100; Vector Lab). All sections were counterstained with Mayer's Hematoxylin (Diapath, C0305) and visualized using a bright-field microscope (Leica DM750).

Western blotting

Cells were seeded in 6-well culture plates (seeding number was adjusted for each cell line to reach optimal confluency by the end of the experiment), treated next day with 1 μmol/L ATRi ceralasertib for 24 hours, 2.5 mmol/L HU for 4 hours, and their combination for 24 hours (HU was added for the last 4 hours of the treatment). Cells were subsequently lysed in using boiling SDS buffer [50 mmol/L Tris-HCl (pH 7.5), 150 mmol/L NaCl, and 1% SDS] to extract total cellular proteins, quantified by the BCA Protein Assay Reagent kit (Thermo Fisher Scientific), and prepared using LDS and Reducing Agent (Invitrogen). Western blot analysis was performed with Enhanced Chemiluminescence System (GE Healthcare) and peroxidase-conjugated secondary antibodies (Amersham). The following primary antibodies were used for Western blotting: anti-phospho-RPA32 (Ser33; Bethyl Laboratories A300-246A; 1:1,000), anti-RPA32 (Abcam AB252861; 1:2,000), anti-RPA32 (S4/S8; Bethyl Laboratories A300-245A; 1:3,000), anti-ATR (Cell Signaling Technology, 13934S; 1:1,000), anti-phospho-CHK1 (Ser345; Cell Signaling Technology, 2348S; 1:1,000), anti-CHK1 (Cell Signaling Technology, 2360S; 1:1,000), anti-phospho-Histone H2AX (Ser139; Cell Signaling Technology, 80312S; 1:1,000), anti-H2AX (Cell Signaling Technology, 7631S; 1:1,000), anti-phospho-DNA-PK (Ser2056; Cell Signaling Technology, 68716S; 1:1,000), anti-DNA-PK (Cell Signaling Technology, 12311S; 1:1,000), anti-RAD51 (Genetex GTX70230; 1:1,000), and anti-HSP90 (Santa Cruz Biotechnology, SC-7947; 1:1,000). In the Western blot screening analysis, we used following antibodies: anti-ATM (Cell Signaling Technology, 2873S; 1:1,000); anti-P53 (Sigma-Aldrich p5813; 1:1,000); anti-RAD51C (Santa Cruz Biotechnology SC-56214; 1:1,000), and anti-Vinculin (MERCK 05-386; 1:3,000). Detection of the chemiluminescent signal was performed with ChemiDoc Imaging System (Bio-Rad).

In vivo xenograft models

Animal procedures were approved by the Ethical Commission of the Institute FIRC of Molecular Oncology (IFOM, Milan, Italy) and by the Italian Ministry of Health, and were performed in accordance with institutional guidelines and international law and policies. Mice were obtained from Charles River and were maintained under pathogen-free conditions in individually ventilated cages and with free access to food and water. During the experiment, investigators were not blinded. Mice were checked daily for signs of illness and distress.

Four- to 5-week-old female NOD-SCID mice were used. Tumor size was measured twice a week and calculated using the formula $V = (d^2 \times D)/2$ (d = minor tumor axis; D = major tumor axis) and reported as tumor volume (mm^3; mean ± SEM of individual tumor volumes).

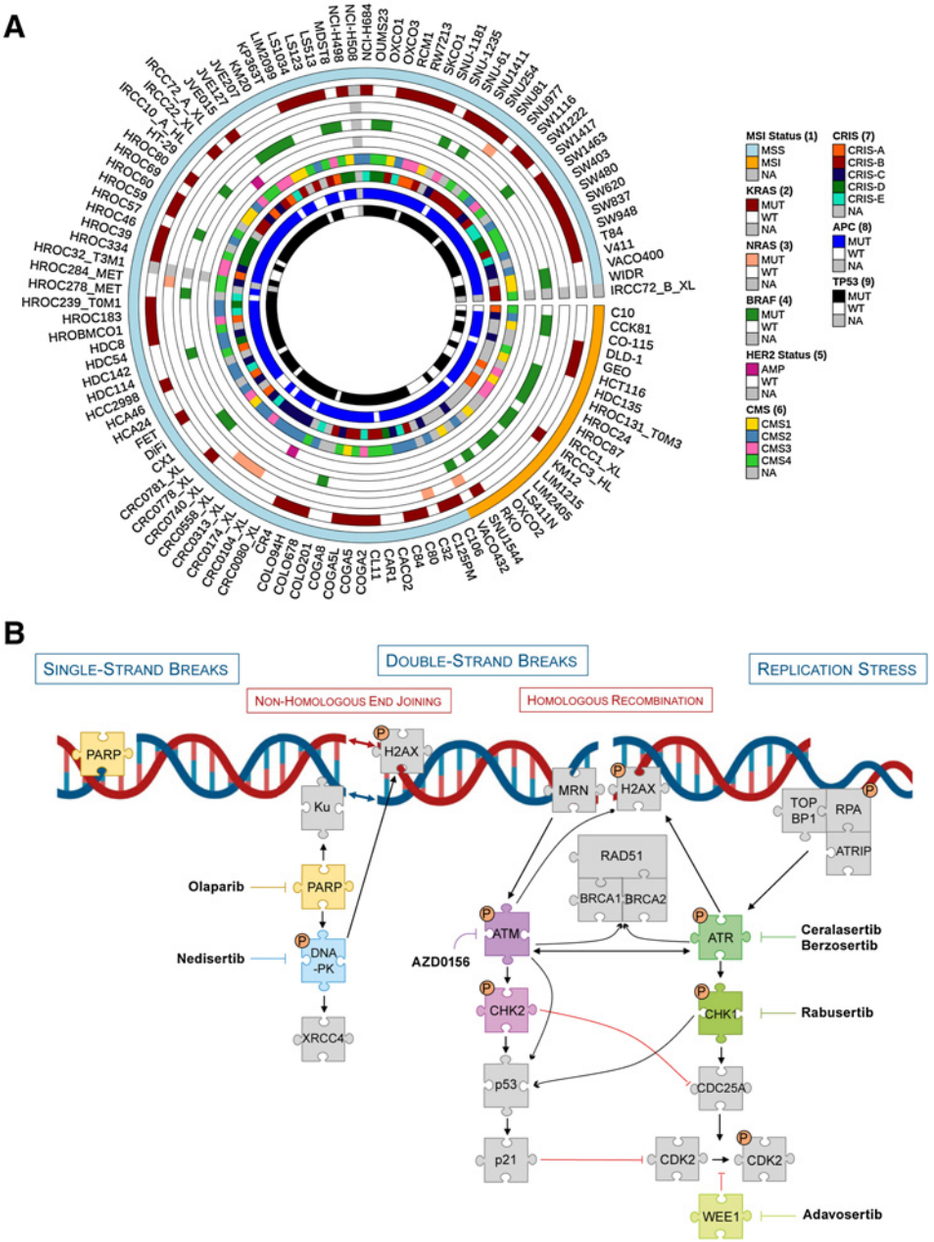

Figure 1.

Selection of cell line models representing the genomic landscape of colorectal cancer and scheme of the DDR pathways with their actionable targets. **A,** Circos plot representing the mutational status of a selected panel of 112 colorectal cancer cell lines enriched for *RAS* and *BRAF* mutations or other alterations conferring resistance to anti-EGFR blockade. The *HER2*, *APC*, and *TP53* genetic status is also reported. The distribution of microsatellite status and representation of transcriptional (CRIS) and molecular (CMS) subtypes in cell lines is also shown. MSS, microsatellite stable; MSI, microsatellite unstable; MUT, mutant; NA, not available; WT, wild type. **B,** Schematic representation with key players of DDR is shown along with the DDRi currently undergoing clinical development.

Exponentially growing C80 cells were resuspended in a mixture of 50% PBS and 50% Matrigel (Corning) and injected subcutaneously in the flank (5×10^6 cells per mouse). Once the tumors reached a volume of approximately 100–200 mm^3, mice were randomized (at least 8 per group) to receive ceralasertib (prepared in 10% DMSO, 40% PEG300, 5% Tween80, and 45% sterile water) or vehicle. The drug solution and the vehicle control were administered by oral gavage daily at 50 mg/kg for 3 weeks.

Statistical analysis

Results were expressed as means ± SEM or SD. Statistical significance was evaluated by unpaired *t* test or Mann–Whitney test as indicated using GraphPad Prism software. $P < 0.05$ was considered statistically significant (*, $P < 0.05$; **, $P < 0.01$; ***, $P < 0.001$; ****, $P < 0.0001$).

Data availability statement

The datasets generated during and/or analyzed during the current study are available from the corresponding author on reasonable request.

Results

Selection of cell line models recapitulating the genomic landscape of colorectal cancer

We previously tested a panel of 99 MSS colorectal cancer cell lines enriched for *KRAS* and *BRAF* alterations and identified

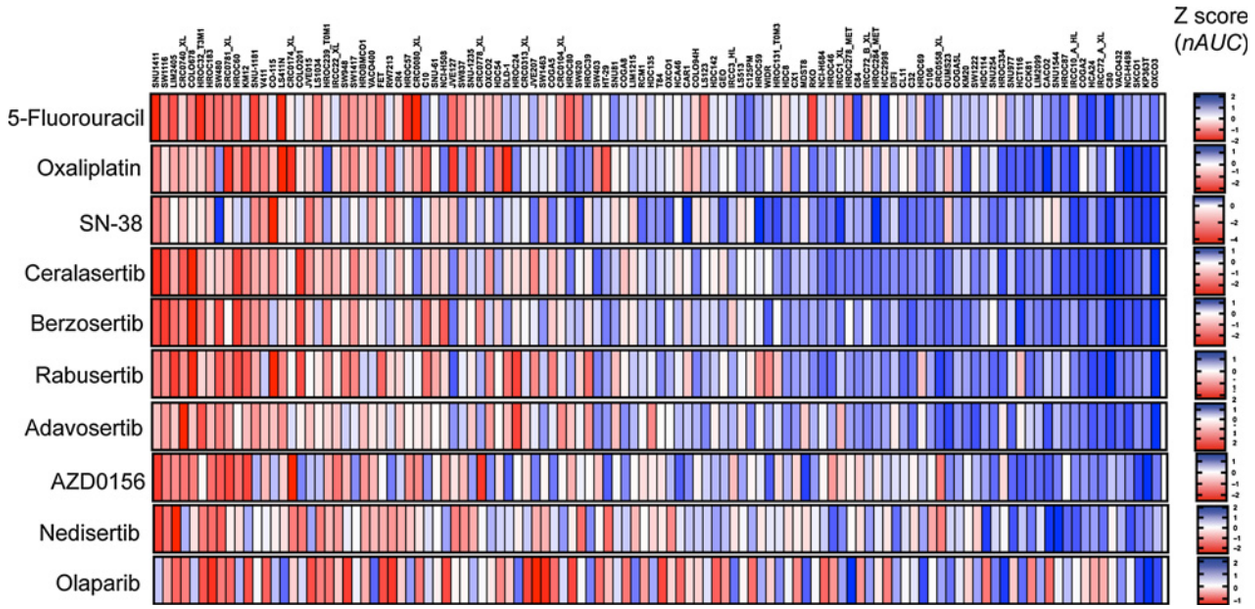

Figure 2.

Response profiles to DDRi and chemotherapeutic agents in colorectal cancer cell models. Heatmap representing pharmacoresponse of 112 colorectal cancer cell lines to three chemotherapeutic drugs and seven different DDRi (two of which target ATR). Cells were treated with monotherapy and cell proliferation was assessed after 7 days of treatment. All experiments were repeated in at least three biological replicates with technical triplicates, and final data are expressed as their average. Viability results were expressed as *Z* scores calculated from normalized AUC (nAUC) values for each individual drug. The red shades represent cells' resistance while the blue scale shows sensitivity to the specific drug. Values for olaparib response have been partly retrieved from our previous publication (12).

a subset of tumors (around 13%) displaying sensitivity to the PARP inhibitor (PARPi) olaparib (12). In this work, we have studied a dataset of 112 cell lines, which include not only the majority of those previously tested with olaparib, but also an additional set of *EGFR/RAS/BRAF/PIK3CA* wild-type and MSI cell lines which were selected to parallel the molecular and transcriptional landscape of colorectal cancer (refs. 39, 40; **Fig. 1A**; Supplementary Table S1). Overall, this panel includes 31 cell lines recently derived from tumor biopsy or surgical colorectal cancer samples, as well as from patient-derived xenografts, for which the clinical annotation is available (refs. 20, 41; **Fig. 1A**; Supplementary Table S1).

Systematic targeting of DDR pathways in colorectal cancer preclinical models

To establish the fraction of colorectal tumors sensitive to DDR pathway inhibitors, we screened colorectal cancer cell lines with drugs targeting key DDR proteins, namely ATM, ATR (two distinct inhibitors), CHK1, WEE1, and DNA-PK (**Figs. 1B** and **2**; Supplementary Fig. S1; ref. 7). For ATR blockade, we employed berzosertib and ceralasertib, because both inhibitors are undergoing clinical development for several solid tumors with varying dosing protocols and administration routes (refs. 17, 42; **Figs. 1B** and **2**; Supplementary Fig. S1).

We also assessed sensitivity to the PARPi olaparib in cell models that were not included in our previous study (ref. 12; **Fig. 2**). In addition, we tested sensitivity of the colorectal cancer cell line platform with the three most used standard-of-care cytotoxic drugs in colorectal cancer, namely, 5-FU, SN-38 (the active metabolite of irinotecan), and oxaliplatin, leading to the identification of additional responsive colorectal cancer cell lines (**Fig. 2**).

Cell-specific and variable levels of response to chemotherapy were noted (**Fig. 2**); an overlapping pattern of response was observed between SN-38 and the ATRi ceralasertib and berzosertib (Spearman correlation $r = 0.52$ and 0.43, respectively; $P < 0.0001$; **Fig. 2**; Supplementary Fig. S2A and S2B).

RS is a targetable vulnerability in colorectal cancer

Drug screening revealed that around 30% of colorectal cancer cell lines were sensitive to DDRi, with 25% of cases being particularly susceptible to ATR inhibition. These values are based on viability <35% at the clinically relevant concentration of 1 μmol/L of the ATRi ceralasertib (**Fig. 2**). Cross-sensitivity to the two ATRi berzosertib and ceralasertib was evident (Spearman correlation $r = 0.78$; $P < 0.0001$), thus validating the screening (Supplementary Fig. S2C). Pathway sensitivity was also maintained with CHK1 and WEE1 inhibition through rabusertib and adavosertib treatment, respectively, thus revealing a broad dependency to the RS pathway in a subset of colorectal cancer models (**Fig. 2**; Supplementary Fig. S3A–S3D).

We considered that ATRi are in advanced clinical development and appear to show effectiveness as monotherapy (18), while ATMi and DNA-PKi appear to be more effective when combined with targeted, radio- or chemo-based therapies (43, 44). Accordingly, we focused on understanding the impact of RS on response to the ATR blockade in colorectal cancer.

We used HU to trigger RS in colorectal cancer cells and we initially assessed pathway activation by immunofluorescence analysis on four ATRi-sensitive and four ATRi-resistant cell lines (Supplementary Fig. S4). We evaluated the role of different DDR effectors on RS, such as γH2AX, a marker of DNA damage (45), activation of replication Protein A (phospho-RPA32), a heterotrimeric

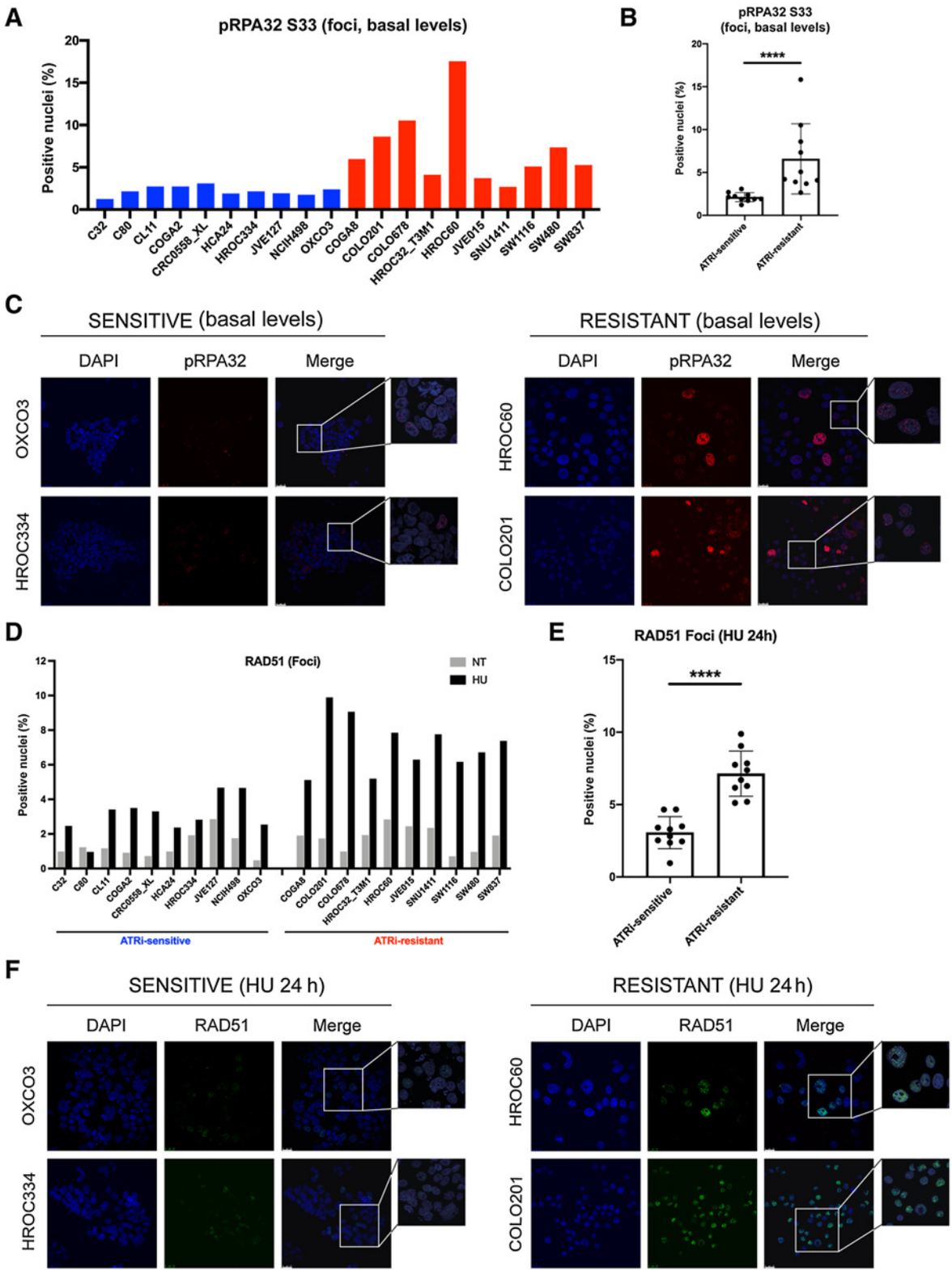

protein which recruits DDR effectors to the damage site to initiate the RS response (46), and the phosphorylated form of CHK1 (pCHK1 S345), a direct ATR target involved in cell-cycle modulation (ref. 47; Supplementary Fig. S4).

Induction of RS by HU triggered DNA damage in both ATRi-sensitive and ATRi-resistant cells, as shown by increased levels of γH2AX and pCHK1 (Supplementary Fig. S4A and S4B). Levels of phosphoS33-RPA32, a residue directly phosphorylated by ATR (48), increased upon HU treatment in both groups (Supplementary Fig. S4C, pan-nuclear signal). We assessed basal levels of pRPA32 foci as an indicator of endogenous RS and we found that ATRi-resistant cells showed significantly higher basal pRPA32 foci with respect to the sensitive cell lines (Supplementary Fig. S4D). Next, we measured RAD51 foci formation upon HU treatment and found that it was significantly increased in ATRi-resistant cells after HU compared with ATRi-sensitive cells (Supplementary Fig. S4E). Intrigued by these findings, we extended the analysis to 16 additional models and performed two independent biological experiments. This analysis confirmed that ATRi-resistant colorectal cancer cells display higher basal levels of pRPA32 foci (**Fig. 3A–C**) and increased levels of RAD51 foci formation upon HU treatment (**Fig. 3D–F**; Supplementary Fig. S5) with respect to ATRi-sensitive cells.

To further evaluate the impact of RS on the DDR signaling pathways, we performed biochemical analysis in cells treated with the ATRi ceralasertib, HU, or their combination (**Fig. 4**). Considering pCHK1 as a marker of ATR pathway activation, we found that this protein was equally activated in ATRi-sensitive and ATRi-resistant lines upon HU treatment, thus mirroring what was previously observed by immunofluorescence assay. However, DNA damage, as assessed by γH2AX accumulation, was already evident upon ATRi treatment only in sensitive cells. In addition, upon 24 hours treatment with ATRi, sensitive cells revealed co-activation of phospho-DNA-PK, further confirmed by measuring RPA32 phosphorylation on S4/S8 residues (49). While S4/S8 residues were already activated upon treatment with single-agent ATRi or HU in ATRi-sensitive cells, these residues were phosphorylated in ATRi-resistant cells only when HU-based treatment was administered. A similar pathway of activation was also observed for pRPA32-S33 residue (**Fig. 4**), highlighting a clear ATR dependency in ATRi-sensitive cells to cope with RS.

Identification of biomarkers of response to ATR pathway inhibitors in colorectal cancer

Predictive biomarkers are needed to stratify patients likely to respond to ATR pathway inhibitors, but research efforts in malignancies other than colorectal cancer have achieved modest results (17, 42). To fill this gap, we initially performed bioinformatic analysis on genomic, RNA-seq, and proteomic data gathered from the colorectal cancer cell lines coupled with pharmacogenomic response to ATM, ATR, CHK1, WEE1, and DNA-PK inhibitors. In addition to *cMYC*, *RAS*, and *cyclin E (CCNE1* and *CCNE2;* Supplementary Figs. S6–S8), whose aberrant activation is known to trigger RS in other tissues (50), we included other genes involved in carcinogenesis and in cell-cycle control (Supplementary Figs. S9 and S10). In general, in our cohort, we could not find any robust and statistically significant correlations between response to ATR pathway inhibitors (ATRi, CHKi) and genomic alterations in the subset of DDR/cell-cycle genes analyzed in colorectal cancer models.

We then evaluated *TP53*, a tumor suppressor gene involved in the cell-cycle control and DDR activation (51). No correlation was found between response to ATRi and genetic alterations of *TP53* defined as functionally relevant according to the p53.iarc.fr database or p53 protein loss (Supplementary Figs. S9, S10, S11A, and S11B).

We next analyzed alterations of the *ATM* gene and loss of ATM protein, which are known to confer sensitivity to ATRi in other tumor types such as prostate and pancreatic cancer (52, 53).

Distribution of SNVs in the *ATM* sequence was not associated with ATRi sensitivity (Supplementary Fig. S9A and S9B), while colorectal cancer cells showing ATM protein loss (tested both by Western blot and IHC analysis) were clearly sensitive to ATRi (**Fig. 5A**; Supplementary Fig. S12A and S12B). This observation was confirmed when we extended the analysis to an additional dataset of 129 colorectal cancer cell lines that are part of our colorectal cancer cell line collection (Supplementary Fig. S12C); indeed, we found that ATM protein loss is invariably associated with sensitivity to ATRi (Supplementary Fig. S12D).

To mechanistically confirm these findings, we used CRISPR-mediated gene editing to generate *ATM* KO in SW480 colorectal cancer cells, which are resistant at the clinically relevant ATRi (ceralasertib) concentration of 1 μmol/L (**Fig. 5B** and **C**). We isolated two independent clones from two different guides (guide 1 and 2, clones 1.4, 1.7, 2.2, and 2.3) and all of them showed sensitivity to ATR inhibition compared with isogenic parental controls, confirming previous work showing that *ATM* is a fundamental player driving DDR and RS response (ref. 54; **Fig. 5D**).

We then considered whether different cell lines that are highly sensitive to PARP inhibition as shown in our previous work (12) were also sensitive to ATR inhibition, suggesting that HR deficiency might also represent a mechanism of sensitivity to RS (Supplementary Fig. S13A). KP363T, HROC334, and HROC278MET exhibited the highest sensitivity to olaparib (12) and were also sensitive to ATRi. Although we were not able to identify potentially pathogenic SNVs in DDR genes in these cells, when we considered RNA-seq and protein analysis we found out that all of them had no or very low levels of RAD51C expression (Supplementary Fig. S13B and S13C), a RAD51 paralog whose loss is a well-known mechanism of PARPi sensitivity in breast and gastric cancer (55). The HROC87 cells which express RAD51 at very low levels (Supplementary Fig. S13D) were also sensitive to ATRi (Supplementary Fig. S13A).

Figure 3.

Cells resistant to ATR inhibition exhibit higher levels of endogenous RS and increased RAD51 activity upon exogenous induction of RS. **A,** Immunofluorescence detection of basal pRPA32 foci in ATRi-sensitive (blue histograms) and ATRi-resistant (red histograms) cell models was performed and quantified (at least 400 nuclei were counted for each cell line in two biological replicates). **B,** Statistical significance for basal pRPA32 foci formation between ATRi-sensitive versus ATRi-resistant cell models was calculated using the Mann–Whitney test. Statistical significance: ****, $P < 0.0001$. **C,** Representative images of immunofluorescence staining of pRPA32 foci at basal levels in two ATRi-sensitive and two ATRi-resistant models. DAPI was used to stain nuclei. Magnification: 40×, scale bar: 25 μm. **D,** ATRi-sensitive and ATRi-resistant cell models were treated with 2.5 mmol/L HU for 24 hours. Following treatment, immunofluorescent detection of RAD51 foci formation was performed and compared with untreated cells. **E,** Statistical significance for RAD51 foci formation upon 24 hours HU treatment between ATRi-sensitive versus ATRi-resistant cell models was calculated using the Mann–Whitney test. Statistical significance: ****, $P < 0.0001$. **F,** Representative images of immunofluorescence staining of RAD51 foci after 24-hour-long treatment with 2.5 mmol/L HU in two ATRi-sensitive and two ATRi-resistant models. DAPI was used to stain nuclei. Magnification: 40×, scale bar: 25 μm. For images from the full experiment, please see Supplementary Fig. S5.

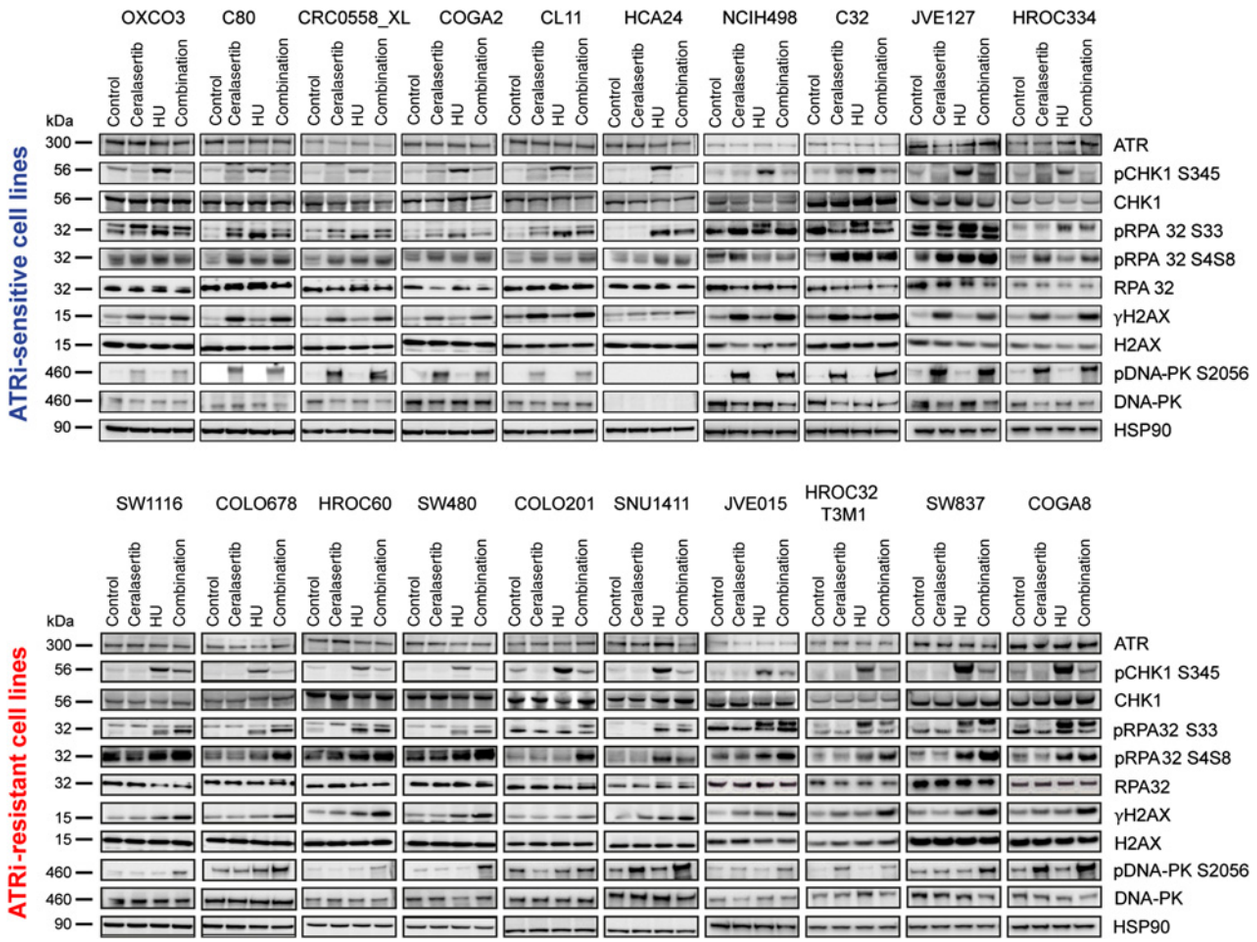

Figure 4.

Cells sensitive to ATR inhibition exhibit higher levels of endogenous RS activation and DNA-PK activation. The expression and phosphorylation of key players in ATR pathway, RS, NHEJ, and DNA damage was measured by Western blot analysis after 24 hours treatment with 1 μmol/L ATRi ceralasertib, 4 hours HU at a concentration of 2.5 mmol/L, or combination of the two agents (20 hours only ATRi followed by 4 hours ATRi+HU). Cell extracts were immunoblotted with the indicated antibodies and HSP90 was used as a loading control.

Analysis of mutational signatures and response to DDRi in colorectal cancer cell lines

Mutational signatures are the imprints of DNA damage and repair processes that are in place over the course of tumorigenesis (56). Several mutational signatures have been shown to be the direct outcome of DNA repair deficiencies and have been proposed as biomarkers of targetable pathway abnormalities (57). To understand whether mutational signatures highlighted sensitivity to ATR inhibition, we undertook whole-genome sequencing of 28 cell lines, choosing among the most ATRi-sensitive and ATRi-resistant cells. Next, we obtained all single-base substitution mutations relative to the reference human genome and performed mutational signature analysis as reported previously (35), and explored relationships with the ceralasertib blockade.

Mutational signature analysis (Supplementary Table S2) revealed four cases with MSI (CO-115, KM12, SNU1544, and VACO432) and one case (HCA24) with alteration in polymerase proofreading. These are well-described DNA repair abnormalities with known potential sensitivities to immune checkpoint therapies and have distinct hypermutator phenotypes. These five samples have the highest tumor mutational burdens within the cohort. Excluding these five cases, we explored mutational signatures of the rest of the cohort and found that cell lines with increased sensitivity to ceralasertib have a significantly higher representation of mutational signatures that are associated with other DNA repair abnormalities in aggregate, including base excision signature 18—associated with damage from 8-oxo-dG (8-Oxo-2′-deoxyguanosine), signature 30 due to NTHL1 deficiency, and signature 36 due to MUTYH loss and HR repair (signatures 3 and 8) deficiencies ($P = 0.0186$). Of note, HRDetect high scores appeared to identify models with high sensitivity to ATR blockade, as HROC278MET, KP363T, and HROC334 exhibited the highest HRDetect scores and were sensitive to this DDRi (**Fig. 5E** and **F**; Supplementary Table S2). Thus, mutational signature analysis may be a useful tool in revealing defective DDR mechanisms in colorectal cancer samples even when a matched normal sample is not available.

Testing DDRi in clinically relevant colorectal cancer models

To extend our findings of putative biomarkers of response to ATRi to more clinically relevant models, we tested DDRi in PDOs in which

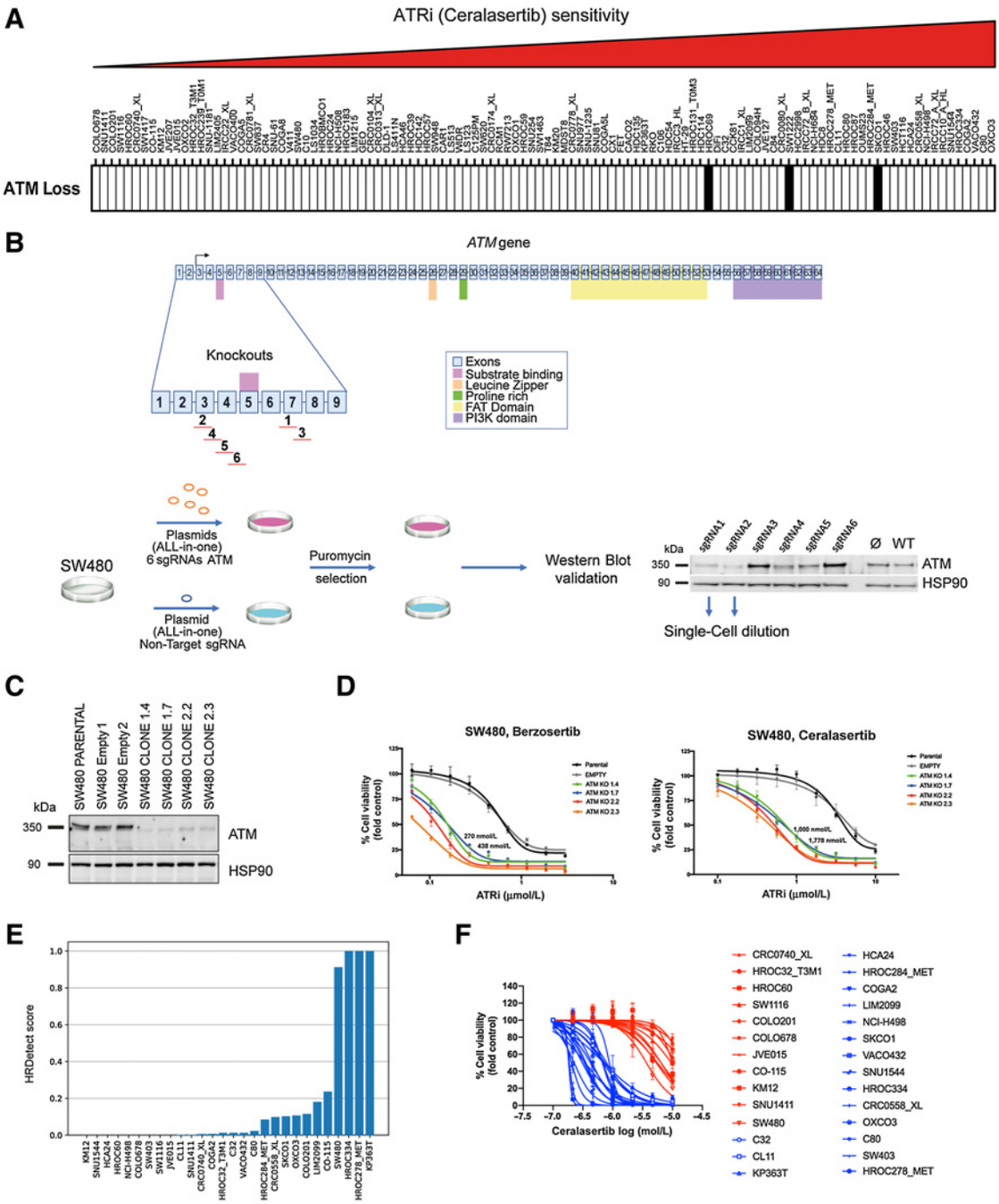

Figure 5.

ATM protein loss and HRDetect analysis identify colorectal cancer models sensitive to ATR inhibition. **A,** Identification of three colorectal cancer cell lines (black bar) with complete ATM protein loss (see Supplementary Fig. S12) and response to ATR blockade by ceralasertib. Colorectal cancer cell lines were ranked based on sensitivity to this ATRi calculated on normalized AUC values. **B,** CRISPR/Cas9 KO of ATM gene by six different sgRNAs targeting different exons in ATRi-resistant colorectal cancer cell line SW480. After puromycin selection of single-cell clones and Western blot validation, clones of sgRNA1 and 2 were selected for further single-cell dilution. **C,** Western blot validation of ATM KOs of four different single-cell clones. SW480 parental cell line and two empty sgRNAs were used as negative controls. HSP90 was used as a loading control of the immunoblotting. **D,** ATRi testing in ATM KO clones by a 7-day-long cell viability assay. Parental cell line SW480 and isogenic SW480 with empty guide were used as controls. Clinically relevant concentration range of inhibitors (around 300 nmol/L in case of berzosertib and around 1,000 nmol/L for ceralasertib) are highlighted. A representative experiment of three independent biological replicates with technical triplicates is shown. **E,** Bar plot representing the HRDetect score of 28 colorectal cancer cell lines ordered from the lowest to the highest score across the *x* axis from left to right. **F,** Ceralasertib viability curves in depicted 28 cell lines from **E** after 7-day-long treatment (data coming from **Fig. 2** and Supplementary Fig. S1). Clinically relevant concentration of 1 µmol/L was used as a cutoff to define sensitive models (viability <35%, in blue) compared with the resistant (viability >75%, in red).

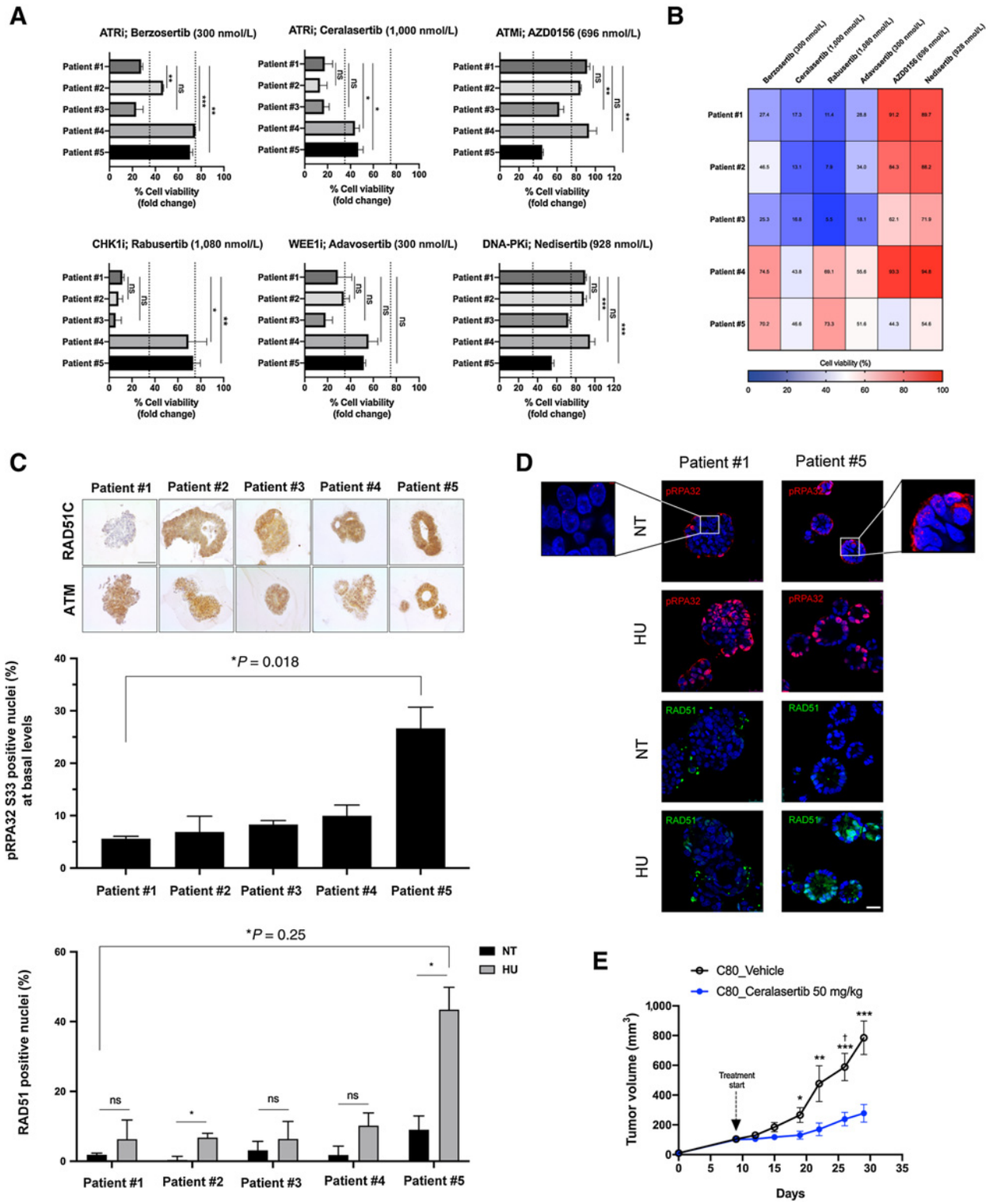

Figure 6.

PDOs and PDXs represent clinically relevant models for determination of sensitivity to DDRi *in vitro* and *in vivo*. **A,** Pharmacologic testing of organoids derived from patients with colorectal cancer with six different DDRi in a 7-day-long viability assay. The results at the endpoint were normalized to control wells containing DMSO vehicle and were plotted as histograms (a percent of viability) at clinically relevant concentrations of individual inhibitors. MG-132 was used as a positive control for organoid death (Supplementary Fig. S14). (*Continued on the following page.*)

sensitivity to olaparib and oxaliplatin had been determined previously (12). Three of five PDOs (Patient #1, #2, #3) were sensitive to ATR pathway inhibition (**Fig. 6A** and **B**; Supplementary Fig. S14). More in general, when comparing these results with sensitivity to FOLFIRI/FOLFOX according to the clinical history of the corresponding patients (Supplementary Table S4 in ref. 12), we found out that these same three organoids were those that previously responded to chemotherapy, thus suggesting that potential DDR deficiency might confer cross-sensitivity to both chemotherapeutics and DDRi. To corroborate the insights gathered from cell line analysis, we performed foci analysis upon HU treatment also in PDOs. We observed concordant results showing lower basal level of pRPA32 foci and RAD51 foci after 24 hours of HU exposure in the ATRi-sensitive models (Patient #1, #2, #3), supporting HR deficiency (12) as a biomarker of response to ATR inhibition, although insufficient to make any solid statistical statement due to the limited size of the cohort (**Fig. 6C** and **D**). Interestingly, the oxaliplatin- and olaparib-sensitive Patient#1 (as characterized in ref. 12), who also responded to previous FOLFIRI treatment, was characterized by loss of RAD51C expression (**Fig. 6C**), suggesting again the loss of this paralog as a putative biomarker of response to both PARPi and ATRi. Patient#4, who showed a pRPA32 and RAD51 profile similar to the ATR-sensitive patients, was resistant to ATRi and PARPi, but sensitive to SN-38 (Supplementary Fig. S15), suggesting that HR-proficient tumors might still be sensitive to topoisomerase I inhibition.

Finally, we assessed the sensitivity to the single-agent ceralasertib *in vivo* using a colorectal xenograft model corresponding to one of the cell lines (C80) that we found sensitive to ATR inhibition in our screening (**Fig. 2**). *In vivo* treatment with ceralasertib led to significant growth control (**Fig. 6E**) and was well tolerated (Supplementary Fig. S16).

Discussion

The last decade has seen an unprecedented opportunity for the development of drugs targeting DDR, and numerous clinical trials are currently assessing their efficacy in various types of malignancies, including colorectal cancer (13, 58). Encouraging results are emerging from different tumors, and development of DDRi in colorectal cancer is confined to investigations in a limited number of preclinical models or in few trials (13, 15, 17), where the identification of robust biomarkers of response still remains an urgent clinical need. Here, we present results obtained from, to our knowledge, the first large-scale screening of colorectal cancer preclinical models with seven different DDRi currently being tested in phase I–III clinical trials. In parallel, to identify potentially relevant translational correlations, we have performed a screening with the three most used chemotherapeutic agents for colorectal cancer treatment (5-FU, SN-38, and oxaliplatin), thus providing a unique platform of response to agents directly targeting DNA or DDR. We selected 112 colorectal cancer cell lines closely recapitulating the genomic landscape of this tumor type, with a specific enrichment for *RAS/BRAF*-mutant models that remain an unmet need in metastatic colorectal cancer due to their unresponsiveness to targeted therapies such as cetuximab or panitumumab. Pharmacologic analysis unveiled that around 30% of the models are sensitive to at least one DDRi, suggesting that severe impairment to the DDR machinery in colorectal cancer cells renders these tumors vulnerable, in particular with respect to ATR pathway inhibitors (18%–25%). Interestingly, we previously showed in a comparable screening that the number of cells showing sensitivity to PARPi is approximately half of that we observed targeting RS response effectors (12), suggesting a higher incidence of RS defects compared with HR, at least in colorectal cancer, that could be further exploited for therapeutic intervention. The linear correlation between sensitivity to SN-38 and ATRi is also of potential clinical relevance. SN-38 is the active metabolite of irinotecan, a standard-of-care drug in metastatic colorectal cancer targeting topoisomerase I (TOP1), which is a crucial component of the DNA replication machinery. This correlation cannot be surprising considering that many of these cell lines are characterized by oncogenic activation that historically has been proven to trigger RS. It derives that inhibition of the RS master regulator ATR has emerged as a top candidate gene for synthetic lethality approaches with TOP1 inhibitors (59) and this supports the design of effective combinatorial strategies involving irinotecan and ATRi (60), testing of which is currently beyond the scope of this article.

Given its pivotal role in the RS response, ATR has become an attractive target for the development of small-molecule inhibitors, and many of them are currently being tested in clinical trials as single agent or in combination with other DNA-damaging agents (17, 42). Understanding the mechanisms and identifying biomarkers that predict response to ATRi would improve patients' stratification and the clinical decision-making process. With this purpose, we have initially focused our investigation on the main players involved in the RS response and found that ATRi-resistant cells exhibit higher basal levels of pRPA32. Previous studies have provided a prognostic significance to RPA1 or RPA2 in different tumor types, including colorectal cancer (61). These and our findings might support the fact that tumors carrying higher levels of RPA could be more tolerant to RS. Given that each cell has a finite pool of RPA for interactions with ssDNA and that ATR recruitment and activation is dependent on this interaction, low levels or exhaustion of RPA might explain the sensitivity of some cancer cells to ATRi (62).

We also found that ATRi-resistant cells expressed significantly higher levels of RAD51 foci upon HU treatment, suggesting that these cells might rely on RAD51 and HR-mediated mechanisms to overcome DNA damage and RS. Interestingly, we observed the same trend in a very limited set of PDOs that we screened with DDRi. Overall, these data might pose the preclinical evidence for testing for pRPA32 foci at basal level in patient tumor biopsy samples or patient-derived models (63) to potentially identify those who could likely respond to ATRi (**Fig. 7**), similarly to other clinical

(*Continued.*) The screening detected strong pattern of sensitivity to ATRi, CHK1i, and WEE1i in 3 patients (#1–3). Sensitivity cutoff was set to 35% and resistance is above 75% viability (indicated with dashed lines). Unpaired Student *t* test was used for statistical evaluation of the results. ns, nonsignificant. **B,** The heatmap with indicated viability values in percentage at the end of the experiment for indicated drug concentrations. Results (**A** and **B**) are an average of at least two independent biological experiments with technical quadruplicates. *Z* factor values varied between 0.74 and 0.94. **C,** IHC detection of RAD51C and ATM protein in colorectal cancer PDOs' cytoclots. Patient #1 displays RAD51C negativity compared with other PDOs, while all *ex vivo* tumor models display ATM positivity. The sections were counterstained with hematoxylin. Scale bar: 50 μm. Quantification of two independent biological experiments performed for detection of pRPA32 S33 foci at basal levels or RAD51 foci after 24-hour-long HU treatment. NT, nontreated. Statistical significance: *, $P < 0.05$; ns, nonsignificant (two-tailed unpaired Student *t* test). **D,** Representative images of immunofluorescence detection of RAD51 and pRPA32 S33 signal in ATRi-resistant (Patient #5) and ATRi-sensitive (Patient #1) organoids treated with 2.5 mmol/L HU for 24 hours. Scale bar: 25 μm. HU, hydroxyurea; NT, nontreated. **E,** ATRi-sensitive C80 cells were injected into NOD-SCID mice to establish a xenograft growth. After expansion and randomization when the tumor volume in individual mice reached 100–200 mm^3, mice started being treated with ceralasertib (50 mg/kg, by oral administration daily) for 21 days. Tumor volumes were measured every 3 days using caliper. †, One mouse from the control group was sacrificed because of tumor growth reaching the endpoint. Bars, ±SE. Statistical significance: *, $P < 0.05$; **, $P < 0.01$; ***, $P < 0.001$ (Mann–Whitney nonparametric test).

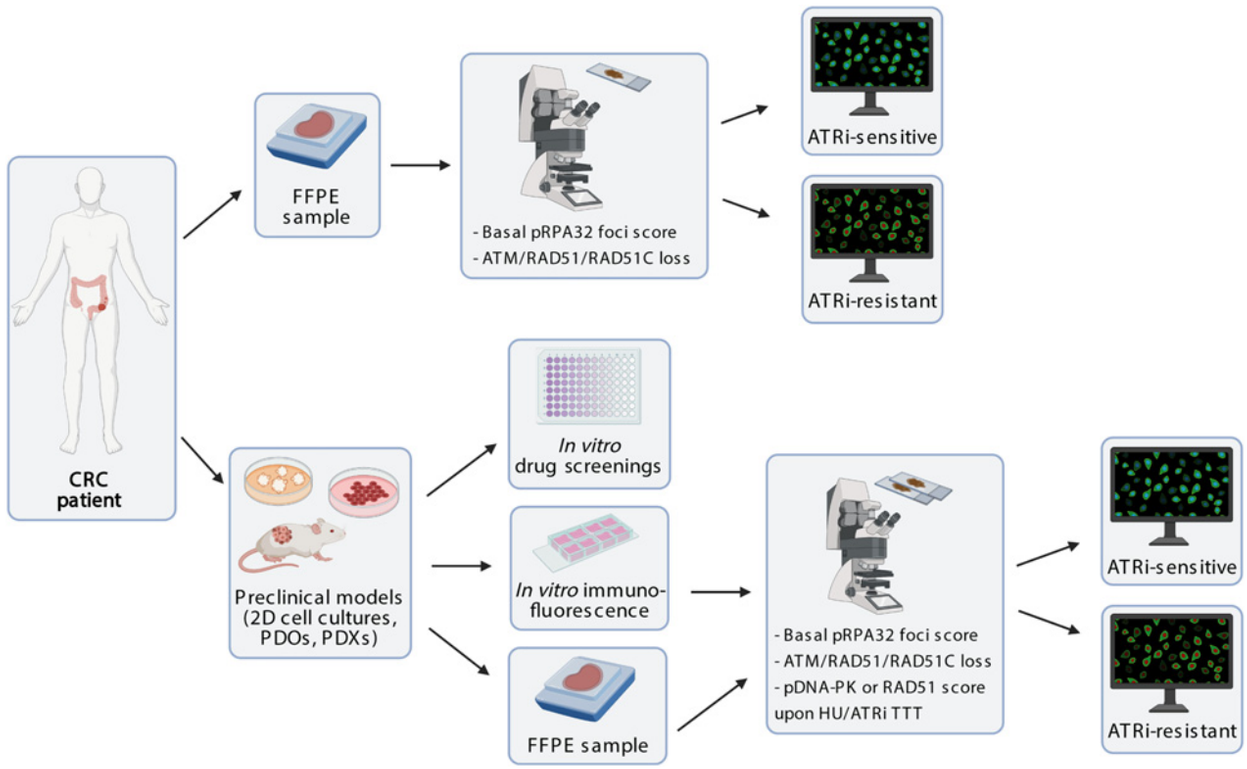

Figure 7.

The proposed preclinical and clinical flow to potentially predict ATRi-sensitive and ATRi-resistant colorectal cancer tumors. After written consent of the patient, tumor sample can be either processed as FFPE sample for direct immunohistologic and immunofluorescence analysis, or preclinical models for *in vitro* and *in vivo* analyses can be established. Samples can be tested for direct *in vitro* drug screenings or for biomarkers analysis through immunofluorescence or IHC assays. To evaluate the relevance of the "composite biomarker" of sensitivity to ATR inhibition, we propose to detect the expression level of proteins ATM, RAD51, and RAD51C together with scoring of phospho-RPA32 at basal level—prior to treatment. Also, scoring of activated DNA-PK and RAD51 upon treatment with ATRi will be informative. This information may eventually lead to the identification of patients who might benefit from ATR inhibition monotherapy, and directly translate the knowledge from bench to bedside. FFPE, formalin-fixed, paraffin-embedded; PDO, patient-derived organoid; PDX, patient-derived xenograft; TTT, treatment. This figure was created with biorender.com.

analyses where RAD51 foci identified PARPi-vulnerable tumors in breast cancer (64).

Considering that genetic data analysis is not sufficient to faithfully predict the real DNA repair capability of a tumor, especially due to the presence of multiple uncharacterized variants of unknown significance, functional testing on a patient-derived platform would be extremely helpful to guide treatment choice, particularly if implemented by the choice of a peculiar clinical setting (13). From a practical point of view, one important limitation of this application could be the difficulty in identifying a clear-cut threshold level to support a yes or no decision for patient selection. An extended analysis in a larger cohort of clinically and molecularly annotated organoids and patients' tumor samples is warranted to translate these findings to a clinical decision level.

Phospho-RPA32 and RAD51 foci levels might be used together with other putative biomarkers that have been previously correlated with sensitivity to ATR inhibition, such as ATM protein loss (52). Accordingly, we propose that analysis of multiple DDR effectors could be combined to generate a "composite" biomarker that more effectively pinpoints patients likely to respond to ATRi (**Fig. 7**). Here we validated the ATM loss as a biomarker of ATRi sensitivity also in colorectal tissue. Because of the prevalence of this alteration [8%–20% (65, 66)] in the colorectal setting, a significant group of patients could potentially benefit from ATRi treatment. Because HR and RS are two closely connected pathways, we reasoned that tumors with HR deficiencies might be cross-sensitive to PARPi and ATRi. Accordingly, cells with ATM loss that in our previous screening resulted sensitive to olaparib (12), and here responded to ATRi, suggest that combination of PARPi with RS response inhibitors might be very effective in colorectal cancer, as also observed in other tissues (6). The same was true also for other models that, by means of transcriptomic analysis, we found having very low expression levels or complete loss of expression of RAD51 or RAD51C—a RAD51 paralog with key functions in HR (67). While RAD51 is an essential gene and many companies are already attempting the development of specific inhibitors, RAD51C remains still untargetable and its loss might identify those patients with colorectal cancer very likely to respond to ATRi, beyond PARP inhibition.

On the practical side, assessment of ATM and RAD51C might result more easily informative respect to the functional evaluation of pRPA32 and RAD51 due to their clear on/off interpretation.

Interestingly, *ATM*, *RAD51*, and *RAD51C* are among the molecular markers that define the *BRCAness* phenotype (also referred to as *HRDness*), and that are evaluated in panel-based companion diagnostic tools used in the clinic to predict HR and to assess patient eligibility for treatment with PARPi (13). More recently, advanced

signature analysis in breast cancer through the HRDetect score has pointed out *RAD51C* loss as a reliable *BRCAness* biomarker (68), suggesting that similar molecular approaches could be attempted in patients with colorectal cancer to further improve patients' selection. Here we have presented HRDetect score analysis performed for the first time without a germline reference in colorectal cancer models. This analysis revealed four cell lines as potential HR defective; three of four were sensitive to ATR inhibition, and interestingly they are characterized by the lack of RAD51C expression. On the other hand, one cell line (SW480) was resistant to the clinically relevant concentration of ceralasertib (1 μmol/L), but showed sensitivity to higher concentrations. Thinking about the limitation to this approach, it should be taken into account that HRDetect is able to identify previous genomic "scars" of HR deficiency that could have evolved during treatment exposure leading to functionally HR-proficient tumor resistant to the therapy (57).

Extended mutational signature analysis further pointed out higher representation of the BER signature in ATRi-sensitive cell lines. Considering the close interconnection between HR and RS pathways, and in particular the role of PARP in cellular processing of DNA damage through the BER pathway (69), we might exploit this genomic analysis together with "composite" biomarker testing to significantly improve and refine patient stratification.

One important limitation of this work is that *in vitro* experiments have been performed keeping preclinical models (cell lines and organoids) in incubators at standard oxygen concentrations (around 20%), which might not completely recapitulate the hypoxic conditions of colorectal cancer tissues; high pO_2 could in fact exert DNA damage that might increase sensitivity to DDRi. However, we were able to show that even at high pO_2 conditions, subsets of very sensitive as well as very resistant models to DDRi could be identified. In addition, our successful testing of single ATRi in a xenograft model has also suggested that preselection for RS sensitivity through the "composite" biomarker analysis might improve efficacy of the treatment, potentially even more if in combination or during sequential treatment with other agents.

In conclusion, we provide preclinical evidence showing the efficacy of novel promising agents targeting DDR and RS in colorectal cancer. Furthermore, we have identified a "composite" biomarker including different effectors of DNA repair deficiency and RS response (basal pRPA32, RAD51 upon HU, ATM loss, and RAD51C loss), and mutational signature analysis as potential predictors of response to specific DDRi and, more broadly, as biomarkers to define distinct class of patients with unique vulnerabilities in the DDR pathways. Further investigation with combinatorial strategies is warranted to maximize DDR-targeting effects in colorectal cancer. These preclinical results could inform future testing of DDRi in selected cohorts of patients suffering from colorectal cancer.

Authors' Disclosures

N.M. Reilly is currently an employee of Cyteir Therapeutics and the entirety of N.M. Reilly's contribution to the submitted work was performed prior to current employment. A. Degasperi reports other support from CRUK outside the submitted work; in addition, A. Degasperi has a patent for HRDetect pending to CRUK. S. Siena reports other support from Agenus, AstraZeneca, BMS, CheckmAb, Daiichi-Sankyo, Guardant Health, Menarini, Merck, Novartis, Roche-Genentech, and Seagen outside the submitted work. A. Sartore-Bianchi reports personal fees from Amgen, Bayer, Novartis, and Servier outside the submitted work. S. Nik-Zainal reports grants from CRUK, Dr Josef Steiner Foundation, and NIHR during the conduct of the study, as well as other support from SABCS outside the submitted work; in addition, S. Nik-Zainal has a patent for HRDetect pending. F. Di Nicolantonio reports grants from Fondazione AIRC, Associazione Italiana per la Ricerca sul Cancro, AIRC under 5 per Mille 2018 (ID. 21091 program) during the conduct of the study, as well as grants from Fondazione AIRC, Associazione Italiana per la Ricerca sul Cancro, AIRC Investigator Grant 21407 and Italian Ministry of Health - TRANSCAN-2 - THRuST outside the submitted work. A. Bardelli reports grants, personal fees, and non-financial support from Neophore; grants from AstraZeneca and Boehringer; personal fees from Illumina and Guardant Health; personal fees and non-financial support from Inivata; and non-financial support from Roche/Genentech global colorectal cancer outside the submitted work. S. Arena reports grants from Fondazione AIRC, Associazione Italiana per la Ricerca sul Cancro, AIRC under MFAG 2017-ID 20236 project, FPRC 5xmille 2017 Ministero Salute PTCRC-Intra 2020 (REGENERATION-YIG 2020 project), and University of Torino, Department of Oncology, Ricerca Locale 2020 and 2021 (premialità pubblicazioni) during the conduct of the study, as well as personal fees from MSD Italia outside the submitted work; in addition, S. Arena has a patent 102022000007535 pending. No disclosures were reported by the other authors.

Authors' Contributions

E. Durinikova: Conceptualization, data curation, formal analysis, validation, investigation, visualization, methodology, writing–review and editing. **N.M. Reilly:** Data curation, validation, investigation, visualization, methodology. **K. Buzo:** Investigation. **E. Mariella:** Data curation, formal analysis, investigation, visualization, methodology. **R. Chilà:** Data curation, investigation. **A. Lorenzato:** Data curation, formal analysis, validation, visualization, methodology. **J.M.L. Dias:** Formal analysis, investigation, methodology. **G. Grasso:** Investigation, visualization. **F. Pisati:** Data curation, formal analysis, visualization, methodology. **S. Lamba:** Investigation, methodology. **G. Corti:** Investigation. **A. Degasperi:** Formal analysis, investigation, methodology. **C. Cancelliere:** Resources. **G. Mauri:** Investigation. **P. Andrei:** Data curation, visualization. **M. Linnebacher:** Resources. **S. Marsoni:** Writing–review and editing. **S. Siena:** Resources, funding acquisition. **A. Sartore-Bianchi:** Resources, funding acquisition. **S. Nik-Zainal:** Data curation, formal analysis, supervision, funding acquisition, methodology, writing–review and editing. **F. Di Nicolantonio:** Funding acquisition, investigation. **A. Bardelli:** Conceptualization, resources, supervision, funding acquisition, writing–review and editing. **S. Arena:** Conceptualization, resources, data curation, formal analysis, supervision, funding acquisition, investigation, visualization, writing–original draft, project administration, writing–review and editing.

Acknowledgments

This work was supported, in part, by Fondazione AIRC under 5 per Mille 2018-ID. 21091 program-P.I. A. Bardelli, G.L. S. Siena, G.L.F. Di Nicolantonio, G.L. S. Marsoni; Fondazione Regionale Ricerca Biomedica Regione Lombardia (Project CP 12/2018 IANG CRC) to S. Siena and A. Sartore-Bianchi; AIRC under MFAG 2017-ID 20236 project-P.I. S. Arena; FPRC 5xmille 2017 Ministero Salute PTCRC-Intra 2020 (REGENERATION-YIG 2020 project) to S. Arena; Ricerca Locale 2020 and 2021 (premialità pubblicazioni)-University of Torino, Dept of Oncology to S. Arena; AIRC IG 2018-ID. 21923 to A. Bardelli.; AIRC IG (no. 20685) to S. Siena; Terapia Molecolare Tumori by Fondazione Oncologia Niguarda Onlus to A. Sartore-Bianchi and S. Siena; International Accelerator Award, ACRCelerate, jointly funded by Cancer Research UK (A26825 and A28223), FC AECC (GEACC18004TAB) and AIRC (22795) to A. Bardelli; Ministero Salute, RC 2020 to A. Bardelli; the project leading to this application has received funding from the European Research Council (ERC) under the European Union's Horizon 2020 research and innovation programme (grant agreement no 101020342) to A. Bardelli; E. Mariella was supported by the FIRC-AIRC "Michele e Carlo Ardizzone" fellowship for Italy. S. Nik-Zainal, A. Degasperi, and J.M.L. Dias are funded by a CRUK Advanced Clinician Scientist Award C60100/A23916, CRUK Early Detection Project award C60100/A27815 and supported by National Institute of Health Research (NIHR) Cambridge Biomedical Research Centre grant BRC-125-20014.

The authors wish to thank V. Costanzo and F. D'Adda di Fagagna (IFOM - the FIRC Institute of Molecular Oncology - Milan, Italy) for their critical reading of the manuscript and insightful suggestions. The authors also thank members of the Molecular Oncology Laboratory at Candiolo Cancer Institute for scientific support and critical reading of the article.

The costs of publication of this article were defrayed in part by the payment of page charges. This article must therefore be hereby marked *advertisement* in accordance with 18 U.S.C. Section 1734 solely to indicate this fact.

Note

Supplementary data for this article are available at Clinical Cancer Research Online (http://clincancerres.aacrjournals.org/).

Received March 18, 2022; revised May 5, 2022; accepted July 1, 2022; published first July 26, 2022.

References

1. Hanahan D, Weinberg RA. Hallmarks of cancer: the next generation. Cell 2011; 144:646–74.
2. Pearl LH, Schierz AC, Ward SE, Al-Lazikani B, Pearl FMG. Therapeutic opportunities within the DNA damage response. Nat Rev Cancer 2015;15: 166–80.
3. Mateo J, Lord CJ, Serra V, Tutt A, Balmaña J, Castroviejo-Bermejo M, et al. A decade of clinical development of PARP inhibitors in perspective. Ann Oncol 2019;30:1437–47.
4. Yap TA, Plummer R, Azad NS, Helleday T. The DNA damaging revolution: PARP inhibitors and beyond. Am Soc Clin Oncol Educ Book 2019;39:185–95.
5. Berti M, Vindigni A. Replication stress: getting back on track. Nat Struct Mol Biol 2016;23:103–9.
6. Ngoi NYL, Pham MM, Tan DSP, Yap TA. Targeting the replication stress response through synthetic lethal strategies in cancer medicine. Trends Cancer 2021;7:930–57.
7. Pilié PG, Tang C, Mills GB, Yap TA. State-of-the-art strategies for targeting the DNA damage response in cancer. Nat Rev Clin Oncol 2019;16:81–104.
8. Rospo G, Lorenzato A, Amirouchene-Angelozzi N, Magrì A, Cancelliere C, Corti G, et al. Evolving neoantigen profiles in colorectal cancers with DNA repair defects. Genome Med 2019;11:42.
9. André T, Shiu KK, Kim TW, Jensen BV, Jensen LH, Punt C, et al. Pembrolizumab in microsatellite-instability-high advanced colorectal cancer. N Engl J Med 2020; 383:2207–18.
10. Di Nicolantonio F, Vitiello PP, Marsoni S, Siena S, Tabernero J, Trusolino L, et al. Precision oncology in metastatic colorectal cancer - from biology to medicine. Nat Rev Clin Oncol 2021;18:506–25.
11. Argiles G, Arnold D, Prager G, Sobrero AF, Van Cutsem E. Maximising clinical benefit with adequate patient management beyond the second line in mCRC. ESMO Open 2019;4:e000495.
12. Arena S, Corti G, Durinikova E, Montone M, Reilly NM, Russo M, et al. A subset of colorectal cancers with cross-sensitivity to olaparib and oxaliplatin. Clin Cancer Res 2020;26:1372–84.
13. Mauri G, Arena S, Siena S, Bardelli A, Sartore-Bianchi A. The DNA damage response pathway as a land of therapeutic opportunities for colorectal cancer. Ann Oncol 2020;31:1135–47.
14. Moretto R, Elliott A, Zhang J, Arai H, Germani MM, Conca V, et al. Homologous recombination deficiency alterations in colorectal cancer: clinical, molecular, and prognostic implications. J Natl Cancer Inst 2022;114:271–9.
15. Manic G, Signore M, Sistigu A, Russo G, Corradi F, Siteni S, et al. CHK1-targeted therapy to deplete DNA replication-stressed, p53-deficient, hyperdiploid colorectal cancer stem cells. Gut 2018;67:903–17.
16. Seligmann JF, Fisher DJ, Brown LC, Adams RA, Graham J, Quirke P, et al. Inhibition of WEE1 is effective in TP53- and RAS-mutant metastatic colorectal cancer: a randomized trial (FOCUS4-C) comparing adavosertib (AZD1775) with active monitoring. J Clin Oncol 2021;39:3705–15.
17. Yap TA, Krebs MG, Postel-Vinay S, El-Khouiery A, Soria JC, Lopez J, et al. Ceralasertib (AZD6738), an oral ATR kinase inhibitor, in combination with carboplatin in patients with advanced solid tumors: a phase I study. Clin Cancer Res 2021;27:5213–24.
18. Barnieh FM, Loadman PM, Falconer RA. Progress towards a clinically-successful ATR inhibitor for cancer therapy. Curr Res Pharmacol Drug Discov 2021;2: 100017.
19. Medico E, Russo M, Picco G, Cancelliere C, Valtorta E, Corti G, et al. The molecular landscape of colorectal cancer cell lines unveils clinically actionable kinase targets. Nat Commun 2015;6:7002.
20. Lazzari L, Corti G, Picco G, Isella C, Montone M, Arcella P, et al. Patient-derived xenografts and matched cell lines identify pharmacogenomic vulnerabilities in colorectal cancer. Clin Cancer Res 2019;25:6243–59.
21. Corti G, Bartolini A, Crisafulli G, Novara L, Rospo G, Montone M, et al. A genomic analysis workflow for colorectal cancer precision oncology. Clin Colorectal Cancer 2019;18:91–101.
22. Soneson C, Love MI, Robinson MD. Differential analyses for RNA-seq: transcript-level estimates improve gene-level inferences. F1000Res 2015;4:1521.
23. Love MI, Huber W, Anders S. Moderated estimation of fold change and dispersion for RNA-seq data with DESeq2. Genome Biol 2014;15:550.
24. Gu Z, Gu L, Eils R, Schlesner M, Brors B. circlize implements and enhances circular visualization in R. Bioinformatics 2014;30:2811–2.
25. Gu Z, Eils R, Schlesner M. Complex heatmaps reveal patterns and correlations in multidimensional genomic data. Bioinformatics 2016;32:2847–9.
26. Li H. Aligning sequence reads, clone sequences and assembly contigs with BWA-MEM; 2013. Available from: http://arxiv.org/abs/1303.3997.
27. Kim S, Scheffler K, Halpern AL, Bekritsky MA, Noh E, Källberg M, et al. Strelka2: Fast and accurate variant calling for clinical sequencing applications. Nat Methods 2018;15:591–4.
28. Chen X, Schulz-Trieglaff O, Shaw R, Barnes B, Schlesinger F, Källberg M, et al. Manta: rapid detection of structural variants and indels for germline and cancer sequencing applications. Bioinformatics 2016;32:1220–2.
29. Sherry ST, Ward MH, Kholodov M, Baker J, Phan L, Smigielski EM, et al. dbSNP: the NCBI database of genetic variation. Nucleic Acids Res 2001;29:308–11.
30. Lappalainen I, Lopez J, Skipper L, Hefferon T, Spalding JD, Garner J, et al. DbVar and DGVa: public archives for genomic structural variation. Nucleic Acids Res 2013;41:D936–41.
31. Hiltemann S, Jenster G, Trapman J, van der Spek P, Stubbs A. Discriminating somatic and germline mutations in tumor DNA samples without matching normals. Genome Res 2015;25:1382–90.
32. Priestley P, Baber J, Lolkema MP, Steeghs N, de Bruijn E, Shale C, et al. Pan-cancer whole-genome analyses of metastatic solid tumours. Nature 2019;575: 210–6.
33. Van Loo P, Nordgard SH, Lingjærde OC, Russnes HG, Rye IH, Sun W, et al. Allele-specific copy number analysis of tumors. Proc Natl Acad Sci U S A 2010; 107:16910–5.
34. Clarke L, Fairley S, Zheng-Bradley X, Streeter I, Perry E, Lowy E, et al. The international genome sample resource (IGSR): a worldwide collection of genome variation incorporating the 1000 Genomes Project data. Nucleic Acids Res 2017;45:D854–D9.
35. Degasperi A, Amarante TD, Czarnecki J, Shooter S, Zou X, Glodzik D, et al. A practical framework and online tool for mutational signature analyses show inter-tissue variation and driver dependencies. Nat Cancer 2020;1:249–63.
36. Tate JG, Bamford S, Jubb HC, Sondka Z, Beare DM, Bindal N, et al. COSMIC: the catalogue of somatic mutations in cancer. Nucleic Acids Res 2019;47:D941–D7.
37. Davies H, Glodzik D, Morganella S, Yates LR, Staaf J, Zou X, et al. HRDetect is a predictor of BRCA1 and BRCA2 deficiency based on mutational signatures. Nat Med 2017;23:517–25.
38. Sanjana NE, Shalem O, Zhang F. Improved vectors and genome-wide libraries for CRISPR screening. Nat Methods 2014;11:783–4.
39. Dienstmann R, Vermeulen L, Guinney J, Kopetz S, Tejpar S, Tabernero J. Consensus molecular subtypes and the evolution of precision medicine in colorectal cancer. Nat Rev Cancer 2017;17:79–92.
40. Isella C, Brundu F, Bellomo SE, Galimi F, Zanella E, Porporato R, et al. Selective analysis of cancer-cell intrinsic transcriptional traits defines novel clinically relevant subtypes of colorectal cancer. Nat Commun 2017;8: 15107.
41. Mullins CS, Micheel B, Matschos S, Leuchter M, Burtin F, Krohn M, et al. Integrated biobanking and tumor model establishment of human colorectal carcinoma provides excellent tools for preclinical research. Cancers 2019;11: 1520.
42. Yap TA, O'Carrigan B, Penney MS, Lim JS, Brown JS, de Miguel Luken MJ, et al. Phase I trial of first-in-class ATR inhibitor M6620 (VX-970) as monotherapy or in combination with carboplatin in patients with advanced solid tumors. J Clin Oncol 2020;38:3195–204.
43. van Bussel MTJ, Awada A, de Jonge MJA, Mau-Sørensen M, Nielsen D, Schöffski P, et al. A first-in-man phase 1 study of the DNA-dependent protein kinase inhibitor peposertib (formerly M3814) in patients with advanced solid tumours. Br J Cancer 2021;124:728–35.
44. Riches LC, Trinidad AG, Hughes G, Jones GN, Hughes AM, Thomason AG, et al. Pharmacology of the ATM inhibitor AZD0156: potentiation of irradiation and olaparib responses preclinically. Mol Cancer Ther 2020;19: 13–25.
45. Bonner WM, Redon CE, Dickey JS, Nakamura AJ, Sedelnikova OA, Solier S, et al. γH2AX and cancer. Nat Rev Cancer 2008;8:957–67.
46. Yates LA, Aramayo RJ, Pokhrel N, Caldwell CC, Kaplan JA, Perera RL, et al. A structural and dynamic model for the assembly of replication protein A on single-stranded DNA. Nat Commun 2018;9:5447.
47. Zhang Y, Hunter T. Roles of Chk1 in cell biology and cancer therapy. Int J Cancer 2014;134:1013–23.
48. Anantha RW, Sokolova E, Borowiec JA. RPA phosphorylation facilitates mitotic exit in response to mitotic DNA damage. Proc Natl Acad Sci U S A 2008;105: 12903–8.

49. Ashley AK, Shrivastav M, Nie J, Amerin C, Troksa K, Glanzer JG, et al. DNA-PK phosphorylation of RPA32 Ser4/Ser8 regulates replication stress checkpoint activation, fork restart, homologous recombination and mitotic catastrophe. DNA Repair 2014;21:131–9.
50. Primo LMF, Teixeira LK. DNA replication stress: oncogenes in the spotlight. Genet Mol Biol 2019;43:e20190138.
51. Lakin ND, Jackson SP. Regulation of p53 in response to DNA damage. Oncogene 1999;18:7644–55.
52. Rafiei S, Fitzpatrick K, Liu D, Cai M-Y, Elmarakeby HA, Park J, et al. ATM loss confers greater sensitivity to ATR inhibition than PARP inhibition in prostate cancer. Cancer Res 2020;80:2094–100.
53. Dunlop CR, Wallez Y, Johnson TI, Bernaldo de Quirós Fernández S, Durant ST, Cadogan EB, et al. Complete loss of ATM function augments replication catastrophe induced by ATR inhibition and gemcitabine in pancreatic cancer models. Br J Cancer 2020;123:1424–36.
54. Khanna KK, Lavin MF, Jackson SP, Mulhern TD. ATM, a central controller of cellular responses to DNA damage. Cell Death Differ 2001;8:1052–65.
55. Min A, Im SA, Yoon YK, Song SH, Nam HJ, Hur HS, et al. RAD51C-deficient cancer cells are highly sensitive to the PARP inhibitor olaparib. Mol Cancer Ther 2013;12:865–77.
56. Alexandrov LB, Kim J, Haradhvala NJ, Huang MN, Tian Ng AW, Wu Y, et al. The repertoire of mutational signatures in human cancer. Nature 2020;578: 94–101.
57. Koh G, Degasperi A, Zou X, Momen S, Nik-Zainal S. Mutational signatures: emerging concepts, caveats and clinical applications. Nat Rev Cancer 2021;21: 619–37.
58. Brandsma I, Fleuren EDG, Williamson CT, Lord CJ. Directing the use of DDR kinase inhibitors in cancer treatment. Expert Opin Investig Drugs 2017; 26:1341–55.
59. Jossé R, Martin SE, Guha R, Ormanoglu P, Pfister TD, Reaper PM, et al. ATR inhibitors VE-821 and VX-970 sensitize cancer cells to topoisomerase I inhibitors by disabling DNA replication initiation and fork elongation responses. Cancer Res 2014;74:6968–79.
60. Thomas A, Pommier Y. Targeting topoisomerase I in the era of precision medicine. Clin Cancer Res 2019;25:6581–9.
61. Dueva R, Iliakis G. Replication protein A: a multifunctional protein with roles in DNA replication, repair and beyond. NAR Cancer 2020;2:zcaa022.
62. Toledo Luis I, Altmeyer M, Rask M-B, Lukas C, Larsen Dorthe H, Povlsen Lou K, et al. ATR prohibits replication catastrophe by preventing global exhaustion of RPA. Cell 2013;155:1088–103.
63. Durinikova E, Buzo K, Arena S. Preclinical models as patients' avatars for precision medicine in colorectal cancer: past and future challenges. J Exp Clin Cancer Res 2021;40:185.
64. Castroviejo-Bermejo M, Cruz C, Llop-Guevara A, Gutiérrez-Enríquez S, Ducy M, Ibrahim YH, et al. A RAD51 assay feasible in routine tumor samples calls PARP inhibitor response beyond BRCA mutation. EMBO Mol Med 2018;10: e9172.
65. Sundar R, Miranda S, Rodrigues DN, Chenard-Poirier M, Dolling D, Clarke M, et al. Ataxia telangiectasia mutated protein loss and benefit from oxaliplatin-based chemotherapy in colorectal cancer. Clin Colorectal Cancer 2018;17:280–4.
66. Grabsch H, Dattani M, Barker L, Maughan N, Maude K, Hansen O, et al. Expression of DNA double-strand break repair proteins ATM and BRCA1 predicts survival in colorectal cancer. Clin Cancer Res 2006;12:1494–500.
67. Sullivan MR, Bernstein KA. RAD-ical new insights into RAD51 regulation. Genes 2018;9:629.
68. Staaf J, Glodzik D, Bosch A, Vallon-Christersson J, Reutersward C, Hakkinen J, et al. Whole-genome sequencing of triple-negative breast cancers in a population-based clinical study. Nat Med 2019;25:1526–33.
69. Horton JK, Stefanick DF, Prasad R, Gassman NR, Kedar PS, Wilson SH. Base excision repair defects invoke hypersensitivity to PARP inhibition. Mol Cancer Res 2014;12:1128–39.